Journal of Nuclear Materials 378 (2008) 17–24

Contents lists available at ScienceDirect

Journal of Nuclear Materials

journal homepage: www.elsevier.com/locate/jnucmat

Influence of silicon on swelling and microstructure in Russian austenitic stainless steel EI-847 irradiated to high neutron doses

S.I. Porollo [a,*], S.V. Shulepin [a], Yu.V. Konobeev [a], F.A. Garner [b]

[a] State Scientific Center of Russian Federation, Institute of Physics and Power Engineering, Obninsk, Russia
[b] Pacific Northwest National Laboratory, Richland, WA, USA

ARTICLE INFO

Article history:
Received 18 September 2007
Accepted 4 March 2008

ABSTRACT

Void swelling and microstructural development of niobium-stabilized EI-847 austenitic stainless steel with a range of silicon levels were investigated by destructive examination of fuel pin cladding irradiated in three fast reactors located in either Russia or Kazakhstan. The tendency of void swelling to be progressively reduced by increasing silicon concentration appears to be a very general phenomenon in this steel, whether observed in simple, single-variable experiments on well-defined materials or when observed in multivariable, time-dependent irradiations conducted on commercially produced steels over a wide range of irradiation temperatures, neutron spectra and dpa rates. The role of silicon on microstructural development is expressed both in the solid solution via its influence on dislocation and void microstructure and via its influence on formation of radiation-induced phases that in turn alter the matrix composition. Surprisingly, increases in silicon level in this study do not accelerate the formation of silicon-rich G-phase, but act to increase the formation of Nb (C,N) precipitates. Such precipitates are known to be associated with delayed void swelling.

1. Introduction

In two reviews by Garner, it was noted that in many experiments silicon is a very effective elemental addition to delay the onset of void swelling during neutron or charged particle irradiation of austenitic stainless steels [1,2]. In simple model alloys the first small amount of silicon actually increases swelling, with larger amounts leading to progressive decreases in swelling, with the peak swelling level of silicon dependent on the Cr and Ni content, displacement rate and irradiation temperature [2]. In more complex structural alloys such a peak has not been observed, however, perhaps because studies have not been conducted with the wider range of small-to-large silicon concentrations normally used in the model alloy studies.

The majority of the available data to support conclusions concerning the effect of silicon on swelling were developed from single variable studies conducted on well-characterized experimental specimens, both simple model alloys and those more complex in composition [1–9]. Such conclusions were not drawn from studies conducted on actual reactor components produced by commercial vendors and which had been irradiated in time-dependent, multivariable reactor environments. To test the general applicability of conclusions concerning the role of silicon under a wide range of both production practices and reactor-relevant environmental conditions, it was decided to examine a range of silicon variations in a frequently used, commercially produced Russian steel used to construct fuel pin claddings that were irradiated in fast reactors located in Russia and Kazakhstan.

In this report are presented results of investigations on the effect of silicon concentration on void swelling and microstructure of commercial heats of austenized, niobium-stabilized stainless steel EI-847 (0.06 C–16Cr–15Ni–3Mo–Nb) irradiated as fuel pin cladding of both regular and experimental fuel assemblies in three fast reactors to neutron doses up to 49 dpa.

2. Materials and methods

The study of the silicon effect on void swelling in the steel EI-847 was carried out on pin claddings of regular and experimental fuel assemblies irradiated in the BOR-60, BN-350 and BN-600 fast reactors where the latter part of the reactor designation specifies the thermal (60) or electrical (350, 600) power in megawatts. Irradiation conditions experienced by the chosen pins are shown in Table 1. Note that there are significant differences in neutron flux-spectra between the three fast reactors, reflecting different sizes of reactor cores and in-core locations, different neutron flux levels and different energy spectra. Note that the neutron spectra in Table 1 become increasingly ‘harder’ moving from BN-600 to BN-350 to BOR-60.

There are also differences in the relative distribution of dose and irradiation temperature along fuel pins in the reactors BOR-60, BN-350 and BN-600 as shown in Figs. 1–3, respectively. A

* Corresponding author.

0022-3115/$ - see front matter © 2008 Published by Elsevier B.V.
doi:10.1016/j.jnucmat.2008.03.027

Table 1
Irradiation conditions for assemblies investigated

#	Assembly	Reactor	Maximum burn-up, % heavy atoms	Maximum neutron fluence, 10^{26} n/m^2, $E > 0.1$ MeV	Maximum dose, dpa	Spectral conversion factor dpa/10^{26} n/m^2
1	P-34	BN-600	6.21	10.7	35	3.3
2	OP-4	BN-350	11.8	10.8	49	4.5
3	OP-3	BN-350	9.84	10.5	48	4.6
4	CC-15T	BN-350	6.0	10.0	46	4.6
5	ZAR-2	BOR-60	10.46	7.29	42	5.8
6	ZAR-8	BOR-60	11.7	7.34	42	5.8
7	BN-6	BOR-60	10.9	6.4	37	5.8

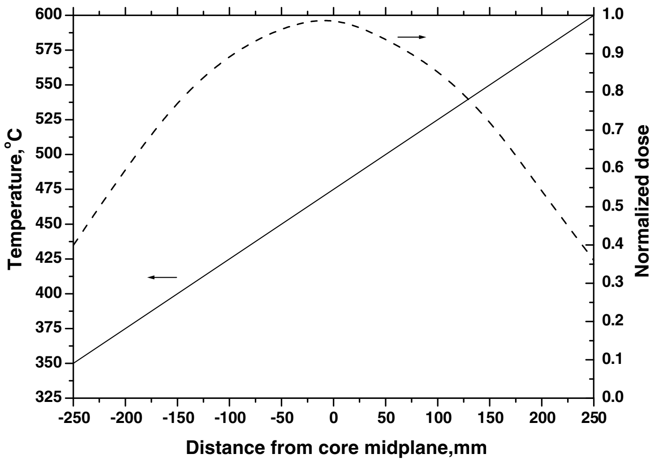

Fig. 1. Relative distribution of dose and irradiation temperature along fuel pins chosen for this study from the BOR-60 reactor.

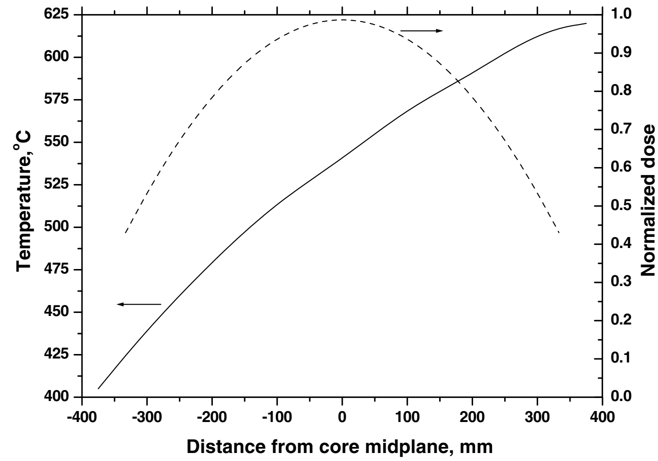

Fig. 3. Relative distribution of dose and irradiation temperature along fuel pins chosen for this study from the BN-600 reactor.

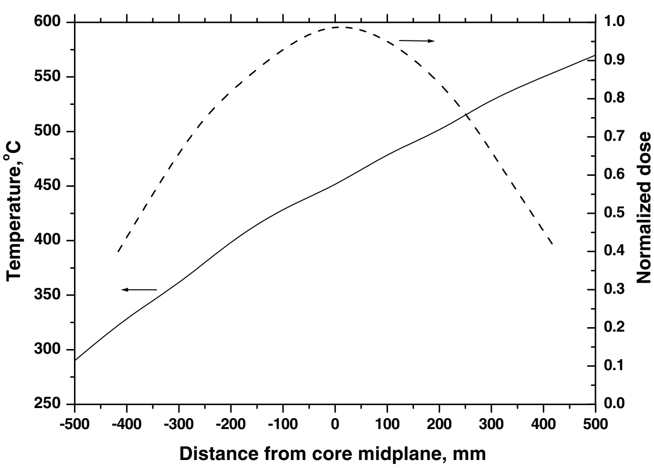

Fig. 2. Relative distribution of dose and irradiation temperature along fuel pins chosen for this study from the BN-350 reactor.

primary determinant of the temperature range in each reactor is the core inlet temperature which varies from ~290 to ~400 °C.

Fuel pin claddings of 6.9 mm outer diameter and 0.4 mm wall thickness were irradiated in each reactor and were made of the EI-847 steel in the austenized condition (1050 °C for 5 min). The chemical composition of all cladding specimens examined corresponded, in general, to the specification requirements for this steel: C(0.04–0.06); Mn(0.4–0.8); Si $\leqslant$ 0.4; S $\leqslant$ 0.010; P $\leqslant$ 0.015; Cr(15.0–16.0); Ni(15.0–16.0); Mo(2.7–3.2); Nb $\leqslant$ 0.9; N $\leqslant$ 0.025; B $\leqslant$ 0.001; Co $\leqslant$ 0.02; Cu $\leqslant$ 0.05; Bi $\leqslant$ 0.01; Pb $\leqslant$ 0.001; Ti $\leqslant$ 0.05, all in wt%. Note that for 'impurity' elements (such as Si, P, N, S) only an upper limit of concentration is specified, thereby allowing some significant swelling-relevant variations in composition in heats produced by different vendors.

After irradiation, segments of 15 mm in length and 4 mm in width were cut from fuel pin cladding at various heights along the pin, from which disks of 3 mm diameter were then punched. From these disks TEM-specimens were prepared using the two-jet 'TENUPOL' polishing technique. The microstructure of the irradiated steel was investigated using a JEM-100CX electron microscope equipped with a lateral goniometer.

Maximum uncertainty in the measurement of mean diameters of voids, dislocation loops and precipitates was equal to 10%. The concentrations and volume fractions of voids and precipitates were measured with an accuracy of 30%. A Kamebax X-ray micro-analyzer was used to measure the composition of the irradiated steels, unless certificates were available that certified the measured composition.

3. Experimental results

3.1. Claddings of BN-600 reactor fuel pins

Thin-wall tubes of 6.9 mm diameter and 0.4 mm thickness fabricated by two western firms from the austenitic stainless steel EI-847 in the austenized condition were used for fuel pin claddings of the first BN-600 core loading. The first post-irradiation examination of these fuel pins began with subassembly P-34 which was irradiated in the low-enrichment zone of the BN-600 core. This subassembly had reached a burn-up of 6.2% heavy atoms. The first examination of the fuel pin bundle in the hot cell after removal of the hexagonal wrapper revealed that the increase of fuel pin length was not uniform, with the pins appearing to exhibit two different

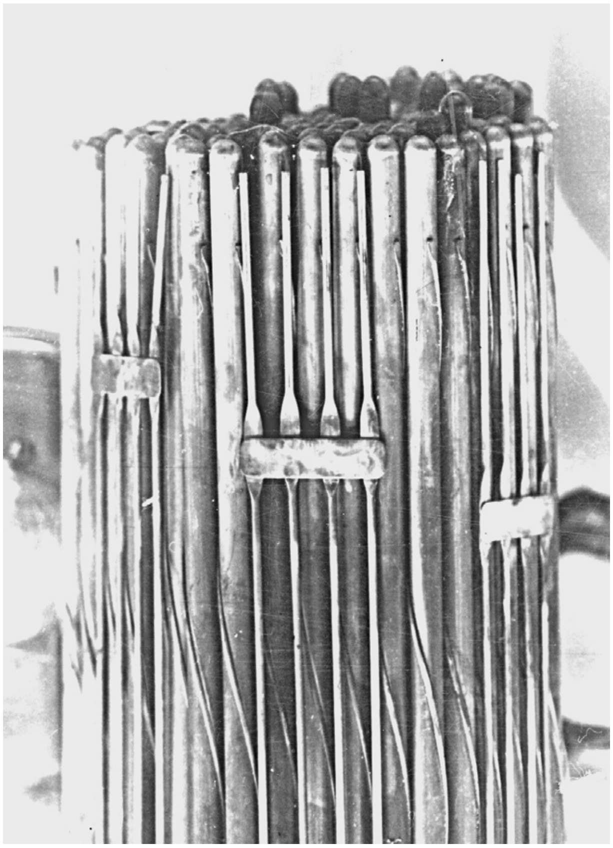

Fig. 4. View of the top end of the fuel pin bundle of the P-34 subassembly [11].

ranges of length (Fig. 4). Measurements of length and diameter confirmed that there were two groups of fuel pins with essentially different changes in dimensions. The location of fuel pins with different length changes appeared to be random across the pin bundle, with no obvious relationship to the orientation of the subassembly in the neutron field or to the temperature distribution.

Therefore it was assumed that different length changes of each set of fuel pins was caused by variations of the chemical composition of EI-847 steel made by different firms. Indeed, an analysis of certificate data for cladding tubes showed that although the chemical composition of each steel made by different firms was within the specification ranges and therefore were essentially identical, their silicon and nitrogen contents varied by a factor of about two, with the largest changes of length and diameter occurring in the steel with the lower silicon content. Nitrogen content has been shown to influence the swelling of austenitic stainless steels [4,5,10] but to a much lesser extent than silicon, so it was assumed that the silicon content was probably the dominant variable influencing swelling in these experiments.

Two fuel pins of subassembly P-34 with larger (#18) and smaller (#122) length changes were selected for further investigation. Using a Kamebax X-ray micro-analyzer the silicon content in these fuel pins was found to be 0.10 ± 0.015 wt% for pin #18 and 0.18 ± 0.011 wt% for pin #122. Certificate specifications for these steels were 0.09 and 0.20% silicon, indicating rather good agreement between the current measurements and certificate data. Nitrogen was experimentally measured at 0.011 and 0.033 wt%, respectively.

The microstructure of both EI-847 lots was similar before irradiation and consisted of a dislocation network with $(6–10) \times 10^{13}\ m^{-2}$ density and Nb(C,N) precipitates with sizes of 50–500 nm and concentrations of $(0.7–2.2) \times 10^{19}\ m^{-3}$. The volume fraction of Nb(C,N) precipitates was equal to ~0.5 %.

Microscopy of claddings of pins #18 and 122 has shown, that after irradiation, voids, dislocation loops, linear dislocations and various types of precipitates are observed with characteristics depending on the irradiation conditions. In Figs. 5 and 6 are shown the void and precipitate microstructures observed at the core center plane. The axial profile of swelling in fuel pins #18 and 122 is shown in Fig. 7, with swelling peaking near the core center.

From Fig. 7 it can be seen that the maximum swelling value for fuel pin #18 cladding is more than three times larger than that of fuel pin #122. This difference in swelling arises primarily from the difference in void size (see Figs. 5, 6 and 8) since the void concentrations are similar in both lots of steel.

The dislocation structure of the irradiated steel EI-847 consists of dislocation loops and a line dislocation network. At irradiation temperatures higher than 500 °C the dislocation density was similar in both steel lots at $\sim 2 \times 10^{14}\ m^{-2}$. The mean diameter of Frank loops in the cladding of fuel pin #18 was approximately twice larger than in fuel pin # 122. In pin #18 the mean loop diameter increased from 42 to 110 nm with increasing irradiation temperature, but in pin #122 it increased from 26 nm to 61 nm.

Fig. 5. Voids and G-phase precipitates observed at the core center plane cross section of fuel pin #18 cladding.

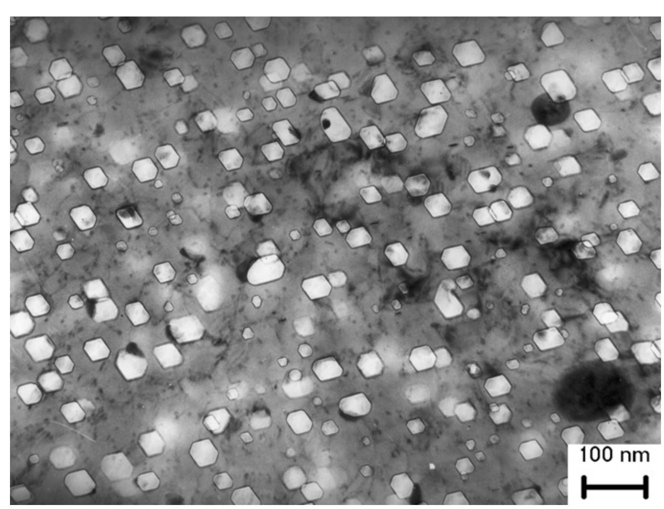

Fig. 6. Voids and precipitates (G-phase and Nb(C,N)) observed at the core center plane of fuel pin #122 cladding.

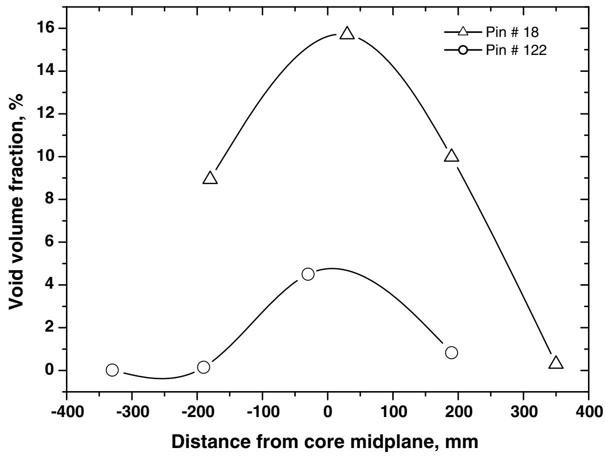

Fig. 7. Axial profile of the void volume fraction in the cladding of fuel pins #18 and #122.

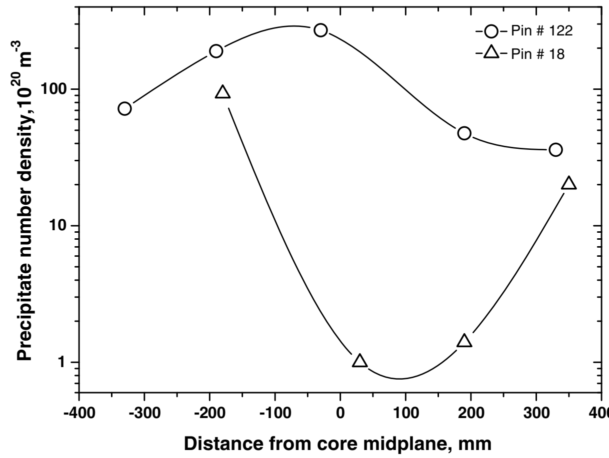

Fig. 9. Axial profiles of the concentration of Nb(C, N) precipitates in cladding from pins #18 and #122 of subassembly P-34.

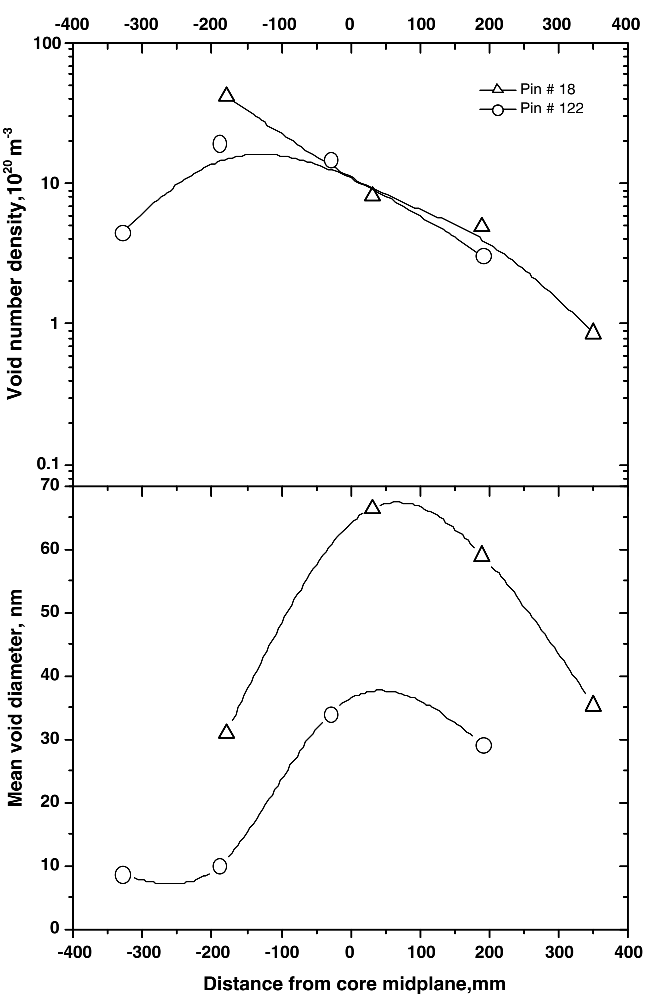

Fig. 8. Axial profiles of mean void diameter and void concentration in claddings of fuel pins #18 and #122.

Several types of the precipitates were observed in the irradiated steel, namely, fine dispersed precipitates of niobium carbonitrides in the bulk of grains, G-phase precipitates, many of which were adjacent to or attached to voids, while Laves phase precipitates were observed in top sections of the fuel pins, and type $M_{23}C_6$ precipitates on grain boundaries. Nb(C,N) precipitates were observed in all fuel pin cross sections investigated. Their size increased slightly with increasing temperature and reached the value of ~10 nm in top sections of the fuel pins. The concentration of these precipitates in fuel pins #18 and #122 changed differently along the axial direction as shown in Fig. 9. In fuel pin #122 the maximum concentration of Nb(C,N) precipitates was observed at the core center plane at 2.7×10^{22} m^{-3}. On the contrary, however, in fuel pin #18 the concentration of these precipitates was minimal at the central plane location and did not exceed $\sim 10^{20}$ m^{-3}.

The most significant precipitation of G-phase was observed in the fuel pin cross sections near the core midplane where the swelling of the cladding was highest. In this case the volume fraction of G-phase in pin #18 was 0.7% (35 nm diameter at 1.3×10^{20} m^{-3}) and was 0.2% (25 nm diameter at1.3×10^{20} m^{-3}) in pin #122.

The microstructure of the fuel pins #18 and #122 cladding was also investigated at the bottom of the pins at a distance of 700 mm below the core midplane where the temperature and dose were 380 °C and 2.8 dpa, respectively. The microstructural characteristics are shown in Table 2 and Figs. 10 and 11.

From these data at 2.8 dpa it can be seen that the higher silicon level not only delayed the onset of void nucleation but was also involved in the evolution of the loop and dislocation microstructure. In the low silicon pin #18 there were small voids and a higher concentration of Frank loops but no line dislocations. In the steel with higher silicon content there were no voids and the Frank loop concentration was significantly lower than in the low silicon steel but line dislocations were present. From these micrographs alone we can not be certain whether the observed line dislocations were remnants of the original population or resulted from unfaulting of some of the Frank loops.

3.2. Fuel pin claddings of the BN-350 reactor

Both regular and experimental subassemblies were irradiated in the BN-350 reactor with fuel pin claddings made from annealed EI-847 steel with various silicon contents. Two subassemblies designated OP-3 and CC-15T are discussed in this report that were irradiated to approximately the same dose but which had fuel pin cladding with certificate-specified silicon levels to be 0.04 and 0.47 wt%, respectively. In Fig. 6 the axial profiles of fuel pin diameter after irradiation in BN-350 to maximum doses of 47.5 and 46 dpa, respectively, are shown.

As seen in Fig. 12, the maximum deformation of irradiated fuel pins corresponds to heights in the range 100–150 mm above the

Table 2
Microstructural characteristics of cladding of pins #18 and #122 at the bottom of the pins

Fuel pin #	$T_{irr.}$, °C	dpa	Voids			Loops		ρ_d, m^{-2}
			d_v, nm	N_v, m^{-3}	$\Delta V/V$, %	d_l, nm	N_l, m^{-3}	
18	380	2.8	8.3	1.9×10^{20}	0.01	32	13×10^{20}	–
122	380	2.8	–	–	–	30	6×10^{20}	6.1×10^{13}

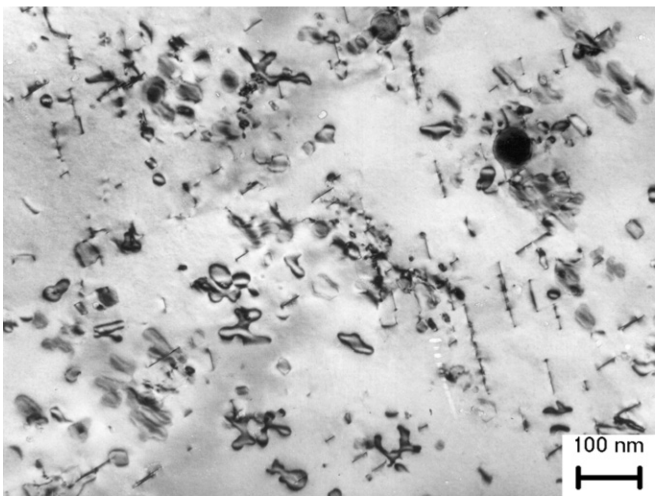

Fig. 10. Microstructure of the cladding of pin #18 at the bottom of the pin (380 °C/2.8 dpa). Note the crenulated nature of the Frank loops at this lower silicon level. The crenulation arises from intersection with very small unidentified precipitates which are visible in loops viewed on edge.

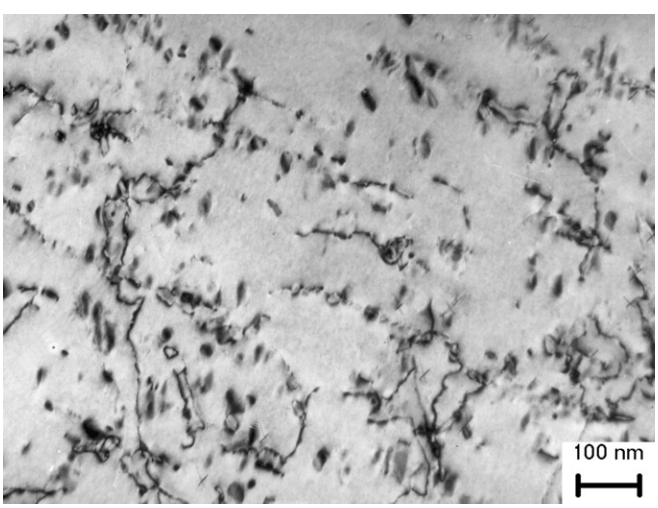

Fig. 11. Microstructure of the cladding of pin #122 at the bottom of the pin (380 °C/2.8 dpa).

core midplane at ~500 °C. The increase in diameter in subassembly OP-3 is almost four times larger than in subassembly CC-15T. Since swelling is the main contribution to the cladding diameter increase and irradiation creep is only a minor contributor for most fuel pins, the maximum swelling of fuel pin cladding in and CC-15T and OP-3 might approach ~4.3% and ~16.9%, respectively. Based on microscopy the maximum swelling appears to be 3.6% and 12.0%, respectively, in relatively good agreement considering the limitations of microscopy on heterogeneously swelling alloys. In Figs. 13 and 14 the mean void diameter and void concentration along the pin length are shown.

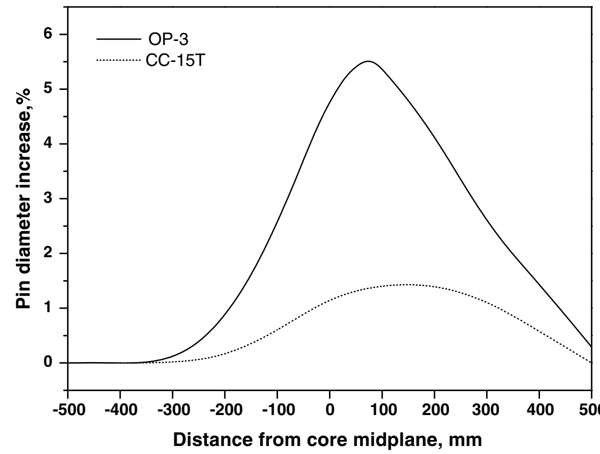

Fig. 12. Axial profiles of fuel pin diameter in the subassemblies OP-3 and CC-15T containing 0.04 and 0.47 wt% silicon, respectively.

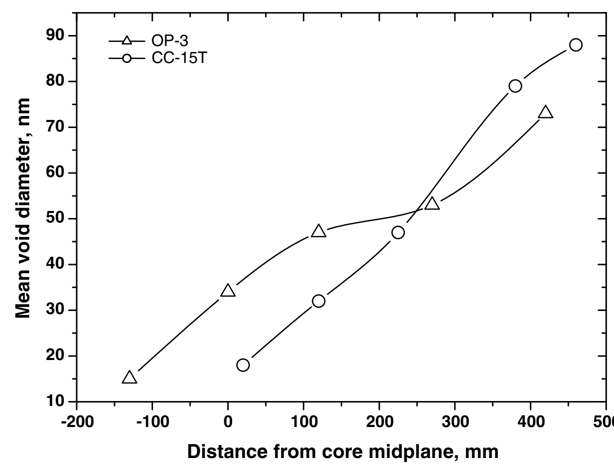

Fig. 13. Axial profile of mean void diameter observed in pins from OP-3 (0.04% Si) and CC-15T (0.47% Si) subassemblies irradiated in the BN-350 reactor.

From Figs. 13 and 14 it follows, that up to the irradiation temperature of 550 °C the void size is larger in the steel with lower silicon content. At higher irradiation temperatures the situation is reversed. Void concentrations in the steel with higher silicon content are less than those of the low silicon steel in the temperature range investigated.

3.3. Fuel pin claddings of the BOR-60 reactor

Two experimental subassemblies (ZAR, BN) with fuel pin cladding made in Russia and various Western firms were irradiated in the BOR-60 reactor. In particular, in the subassemblies ZAR-8 and BN-6 the fuel pin cladding constructed from austenized EI-847 steel with certificate-specified silicon contents of 0.1 and 0.4 wt%, respectively, were irradiated under almost identical conditions. The variation of swelling (measured by electron microscopy) along fuel pin length for these subassemblies is shown in Fig. 15.

From Fig. 15 it is seen that the swelling of low silicon EI-847 steel is significantly higher, and the maximum of swelling of both pins is located just below the core center plane at approximately the same temperature.

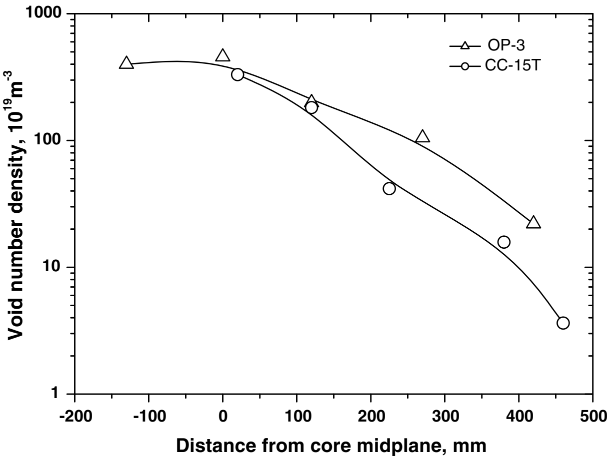

Fig. 14. Axial profile of void concentration observed in fuel pins from OP-3 (0.04% Si) and CC-15T (0.47% Si) subassemblies irradiated in the BN-350 reactor.

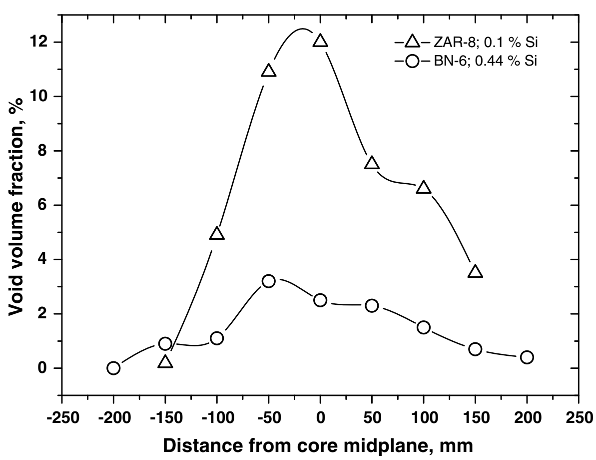

Fig. 15. Axial profile of void volume fraction measured by microscopy in fuel pin cladding of the subassemblies ZAR-8 and BN-6 irradiated in the BOR-60 reactor.

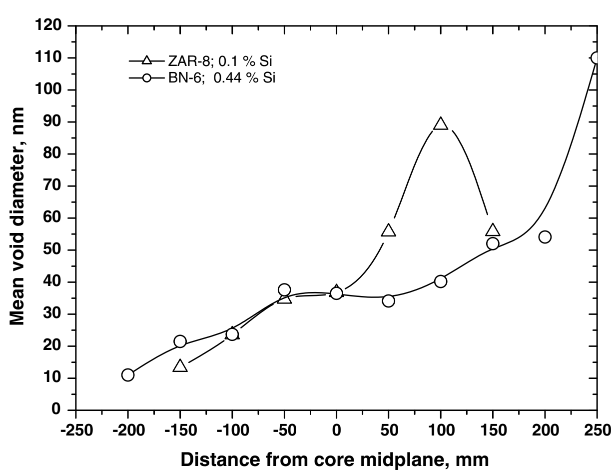

Fig. 16. Axial swelling profiles of the mean void diameter of fuel pins from subassemblies ZAR-8 and BN-6 irradiated in the BOR-60 reactor.

In Figs. 16 and 17 are shown the variations of mean void diameter and void concentration along the axial length of fuel pins from subassemblies ZAR-8 and BN-6 irradiated in BOR-60. In general it appears that the relationship between void size and concentration is a little more complex than observed in the other two data sets presented previously.

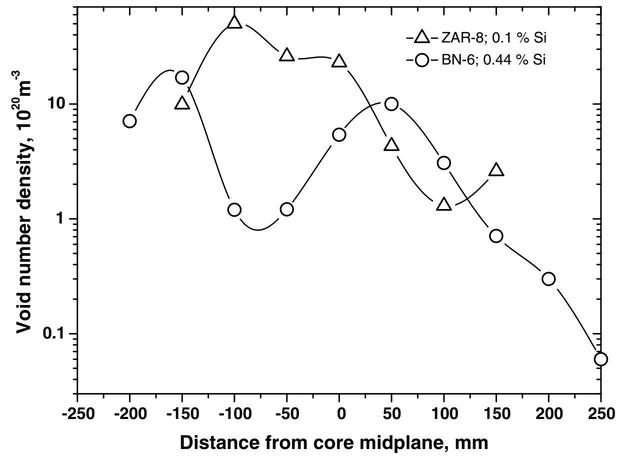

Fig. 17. Axial swelling profiles of the void number density of fuel pins from subassemblies ZAR-8 and BN-6 irradiated in the BOR-60 reactor.

4. Discussion

The results presented above provide evidence of a significant influence of silicon on void swelling in fuel pin claddings fabricated from stainless steel EI-847 regardless of vendor production technology or reactor irradiation conditions. Since the three sets of fuel pins investigated were irradiated over different temperature ranges and at different dose and dose rates it is difficult to make a direct comparison between the three data sets. Therefore in Fig. 18 the average swelling rate (swelling divided by the total dose) is plotted to show the dependence of swelling on silicon concentration near the swelling peak over the dose range of 35–49 dpa at temperatures of 485–550 °C. As shown in Fig. 18 the average swelling rate over this range decreases continuously over the silicon range investigated, regardless of the neutron spectrum or dpa rate.

These data are plotted vs. certificate-specified silicon levels and include not only the six pins presented in this report but also from four other pins with slightly different silicon levels, with all data taken from the assemblies listed in Table 1.

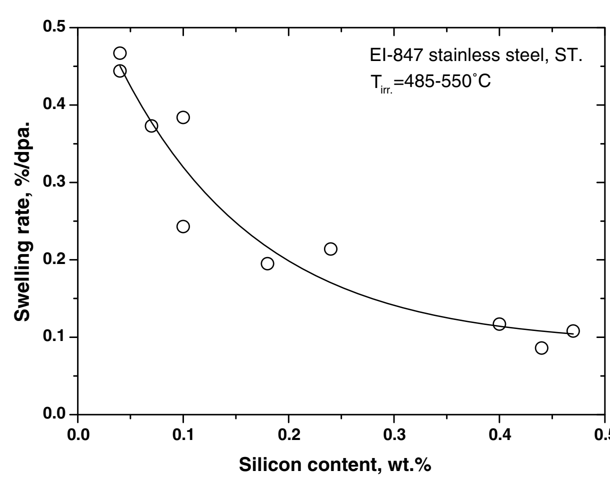

Fig. 18. Dependence of average swelling rate in solution treated EI-847 on silicon content in the range of 35–49 dpa and 485–550 °C.

As presented earlier the general features of silicon's influence on swelling of austenitic stainless steels are known primarily from single-variable experiments involving either neutron or charged particle irradiation [1–9,11–21]. In the majority of published studies it appeared that swelling decreased monotonically with increasing silicon. Other studies conducted on simple Fe–Cr–Ni–Si quaternary alloys that included relatively low silicon levels, however, showed more complicated swelling behavior. As noted earlier, in simple model alloys the swelling actually increases somewhat with small silicon levels before decreasing at higher silicon concentrations. With the exception of the data in Fig. 15 at −150 mm there is no suggestion of such dependence in the more complex alloy series examined in the current study. Unfortunately there are no data in Fig. 18 at <0.04% to confirm or refute the possibility of a peak at very low silicon, and it must be concluded that such low-silicon peaks may be precluded by the action of other solutes in more complex alloys.

It has also been shown that at very high silicon levels the austenite matrix becomes unstable as precipitation of nickel-silicide phases remove sufficient nickel from the matrix to produce lower-swelling ferrite, leading to first an increase and then a reduction of swelling with increasing concentration [5,15,19]. Such behavior was not observed in the concentration range explored by these irradiation experiments.

The influence of silicon on swelling probably occurs by many, often interconnected mechanisms. First, by interacting with point defects formed under irradiation, silicon atoms in the solid solution are known to change the mobility of both interstitials and vacancies and thereby change the diffusion of point defects to sinks [22,23]. The first increase of swelling at low silicon levels has been ascribed to silicon-interstitial binding [22], leading to enhanced formation of Frank interstitial loops similar to the behavior observed for small additions of phosphorus [24]. The subsequent decrease of swelling at higher concentrations has been ascribed to silicon-enhanced diffusivity of vacancies [23], leading to lower vacancy supersaturation and void nucleation, as was also seen with higher phosphorus additions.

The well-known radiation-induced segregation of silicon at defect sinks (grain boundaries, voids, loops and line dislocations, etc.), probably changes the absorption ability of these sinks. It has also been suggested that void growth may be enhanced by the growth of G-phase or other phases connected to void surfaces via a phenomenon designated the 'collector effect' [25].

And finally, the process of solid solution decomposition and the formation of radiation-induced precipitates may be altered by progressive increases in silicon content and by its interactions with other solutes such as phosphorus and carbon. The radiation-induced phases usually remove not only silicon but also nickel from the matrix, with both elements known to strongly influence the onset of void swelling [1]. The identity, composition and volume of these phases vary with irradiation temperature, dpa rate, thermal-mechanical starting condition and concentration of other solutes. Surprisingly, and contrary to expectation, higher silicon levels in this steel appear to increase the stability of the Nb(C,N) phase and retard somewhat the formation of the silicon-rich G-phase.

Two types of silicon influence on the swelling of EI-847 steel are presented in this paper. The first type is illustrated by the low temperature, low dose and dose rate case shown in Figs. 9 and 10. At low irradiation temperatures no easily resolvable precipitates were formed. So, the influence of silicon on void formation must arise primarily from the interaction of Si atoms with point defects, leading to changes in mobility and annihilation of preexisting dislocations, and changes in the density and morphology of Frank loops. Under low temperature irradiation the preexisting dislocations have almost disappeared at 2.8 dpa in the steel with the low silicon content, concurrent with formation of voids and high concentrations of Frank loops. In the higher silicon steel both annihilation of initial dislocations and loop nucleation appear to have been slowed, resulting in an increase in the incubation period of void formation.

The second type of silicon influence is illustrated by the higher-flux, higher-temperature irradiations conducted in BN-600. At 500 °C the influence of silicon leads to decreasing void sizes and insignificant change of void concentration, i.e. silicon appears to suppress the growth of voids rather than depressing void nucleation, although significant differences in phase stability at different silicon levels appear to be involved. In the low silicon steel only G-phase precipitates were present, with a volume fraction of 0.7%. In the steel with higher Si content the volume fraction of G-phase was only 0.2%, but a high concentration of small Nb (C,N) precipitates was observed.

In this work the chemical composition of G-phase precipitates was not determined. Williams and coworkers showed that the composition of G-phase in neutron irradiated steel FV-548 (a close analogue of steel EI-847) was determined to be $Nb_6Ni_{16}Si_7$ [26]. If we postulate that silicon reduces the swelling only when it is in the solid solution, the precipitation of silicon-rich G-phase is certainly an undesirable process, leading to a lowering of both silicon and nickel from the matrix. In addition, G-phase also depletes the solid solution of niobium, making it more difficult to form Nb(C,N) precipitates which are known to be associated with resistance to swelling [26,27].

It is not necessary to have Nb in the alloy to form G-phase, however. Lee [3], Zinkle [28] and Yang [29,30] and their coworkers have shown that Ti-stabilized stainless steels can form these silicon and nickel-rich phases and that their formation is usually concurrent with the onset of swelling.

The relationship between phase stability and void swelling is known to be rather complicated, even in very simple one-variable experiments, and it has been argued by Zinkle et al. [28], as well as many others, that an effective approach to extending the void swelling incubation regime is to inhibit the formation of radiation-induced phases such as G-phase and to encourage the formation of the thermally stable phases such as MC by minimizing the Si concentration. Obviously, the situation is even more complicated than previously imagined, and may be different between Ti-modified and Nb-modified stainless steels. Perhaps the difference also arises from the more complex environmental histories explored in this study. At this time there is insufficient information to define the mechanisms by which increases in silicon in EI-847 steel retard the formation of G-phase.

The most important conclusion derived from this study is that silicon additions to EI-847 steel in the 0.04–0.5 wt% range progressively lower the swelling across a broad range of temperature, dose and dose rate conditions found in fuel pin cladding in three fast reactors.

5. Conclusions

The investigation of neutron-induced void swelling and microstructure of the annealed EI-847 steel with different silicon contents after neutron irradiation to doses in the range of 35–49 dpa at temperatures from 280 to 650 °C leads to the following conclusions.

1. The tendency of void swelling in EI-847 to be progressively reduced by increasing silicon concentration in the range 0.04–0.5wt% appears to be a very general phenomenon in this steel, whether observed in simple single-variable experiments on well-defined materials or in multi-variable, time-dependent

irradiations conducted on commercially produced steels over a wide range of time-varying irradiation temperatures, neutron spectra and dpa rates.

2. The swelling of the steel at irradiation temperatures 485–550 °C is markedly reduced with increasing silicon content. The most appreciable reduction is observed at Si contents in the range from 0.04 to 0.20 wt% with further increases in Si content influencing swelling somewhat less strongly.
3. Although an initial increase in swelling is often observed in simple model austenitic alloys with small additions of silicon, such a swelling peak with increasing silicon addition was not observed in EI-847, possibly as a result of the combined influence of other solutes in this more complex alloy.
4. Under low dose and dose rate conditions at 380 °C the influence of silicon on the microstructural evolution in the steel EI-847 reveals itself by slowing down the processes of annihilation of preexisting dislocations and Frank loop formation.
5. At temperatures in the 485–550 °C range and at high doses and dose rates the swelling is affected by silicon not only by its action in the solid solution but by its influence on the formation of precipitates. Surprisingly and contrary to expectations, higher silicon levels promote stability of Nb(C,N) precipitates and retard the formation of G-phase precipitates known to be enriched in both silicon and nickel. The delayed removal of these elements from solution is probably the major reason why swelling is retarded at higher silicon levels.

Acknowledgements

This work was supported by the Russian Foundation for Basic Research under Projects #07-02-01353 and #07-08-13642 ofi-c. The participation of F. A. Garner was supported by the US department of Energy, Office of Fusion Energy Sciences under Contract DE-AC06-76RLO at Pacific Northwest National Laboratory.

References

[1] F.A. Garner, Irradiation performance of cladding and structural steels in liquid metal reactors, Materials Science and Technology: A Comprehensive Treatment, vol. 10A, VCH Publishers, 1994 (Chapter 6).
[2] F.A. Garner, A.S. Kumar, in: F.A. Garner, N.H. Packan, A.S. Kumar (Eds.), Effects of Radiation on Materials: Thirteenth International Symposium (Part 1) Radiation-Induced Changes in Microstructure, ASTM STP 955, ASTM, Philadelphia, PA, 1987, p. 289.
[3] E. Lee, A. Rowcliffe, E. Kenik, J. Nucl. Mater. 83 (1979) 79.
[4] J.F. Bates, in: Properties of Reactor Structural Alloys after Neutron of Particle Irradiation, ASTM STP-570, 1975, p. 369.
[5] J.F. Bates, R.W. Powell, E.R. Gilbert, in: Effects of Radiation on Materials: 10th Conference, ASTM STP-725, 1981, p. 713.
[6] J.F. Bates, W.G. in: AIME International Conference on Radiation Effects on Breeder Reactor Structural Materials, Scottsdale, AZ, 1977, p. 625.
[7] G.R. Gessel, A.F. Rowcliffe, The effect of solute additions on the swelling of an Fe-7.5Cr-20Ni alloy, in reference 6, p. 431.
[8] F.A. Garner, H.R. Brager, J. Nucl. Mater. 155–157 (1988) 833.
[9] C. Brown, V. Levy, J.L. Seran, K. Ehrlich, R.J.C. Roger, H. Bergmann, in: Proceedings of International Conference on Fast Reactors and Related Fuel Cycles, vol. 1, Kyoto, Japan, 1991, p. 7.5-1.
[10] N. Igata, Y. Kohno, N. Tanabe, F. Rotman, H. Tsunakawa, in: Proceedings of Seventh International Conference on High Voltage Electron Microscopy LBL-16031, August 16–19, 1983, p. 187.
[11] F.G. Reshetnikov, F.M. Mitenkov, M.F. Troyanov, Atomnaya. Energiya. 70 (2) (1991) 104.
[12] V.N. Bykov, V.D. Dmitriev, S.I. Porollo, Fiz. Met. Metalloved. 61 (6) (1986) 1140.
[13] D.J. Mazey, D.R. Harries, J.A. Hudson, J. Nucl. Mater 89 (1980) 155.
[14] M.J. Makin, G.P. Walters, R.N. Singh, T. Leffers, in: Proceedings of Irradiation Behavior of Metallic Materials for Fast Reactor Core Components, Ajaccio, France, 1979, p. 196.
[15] H.R. Brager, F.A. Garner, in: Proceedings of AIME Symposium on Irradiation Phase Stability, Pittsburgh, PA, 1980, p. 219.
[16] H.R. Brager, F.A. Garner, J. Nucl. Mater. 73 (1978) 9.
[17] N. Sekimura, F.A. Garner, J.W. Newkirk, J. Nucl. Mater. 191&194 (1992) 1244.
[18] H. Watanabe, F.A. Garner, T. Muroga, N. Yoshida, J. Nucl. Mater. 225 (1995) 76.
[19] R.M. Boothby, T.M. Williams, G.C. Bromly, Mater. Nucl. Core Appl., BNES (1987) 223.
[20] T.M. Williams, R.M. Boothby, J.M. Titchmarsh, Mater. Nucl. Core Appl., BNES (1987) 293.
[21] H. Watanabe, F. A. Garner, in: M.L. Hamilton, A.S. Kumar, S.T. Rosinski, M.L. Grossbeck (Eds.), Effects of Radiation on Materials: 19th International Symposium, ASTM STP 1366, American Society for Testing and Materials, 2000, p. 859.
[22] F.A. Garner, W.G. Wolfer, J. Nucl. Mater 102 (1981) 143.
[23] B. Esmailzadeh, A.S. Kumar, F.A. Garner, J. Nucl. Mater. 133&134 (1985) 590.
[24] H. Watanabe, A. Aoki, H. Murakami, T. Muroga, N. Yoshida, J. Nucl. Mater. 155&157 (1988) 15.
[25] L.K. Mansur, Phil. Mag. A44 (1981) 86.
[26] T.M. Williams, J.M. Titchmarsh, D.R. Arkell, J. Nucl. Mater. 107 (1982) 222.
[27] N.M. Mitrofanova, F.G. Reshetnikov, Yu.K. Bibilashvili, M.G. Bogolepov, V.P. Voeykov, A.V. Tschelischev, I.M. Neklyudov, V.N. Voyevodin, in: Proceedings of 5th Conference on Reactor Materials Science, Dimitrovgrad, vol. 2, 1998, p. 99 (Part 2, in Russian).
[28] S.J. Zinkle, P.J. Maziasz, R.E. Stoller, J. Nucl. Mater. 206 (1993) 266.
[29] W.J.S. Yang, H.R. Brager, F.A. Garner, in: Proceedings of AIME Symposium on Irradiation Phase Stability, Pittsburgh, PA, October 5–9, 1980, p. 257.
[30] W.J.S. Yang, in: F.A. Garner, N.H. Packan, A.S. Kumar (Eds.), Radiation-Induced Changes in Microstructure: 13th International Symposium, ASTM STP 955, American Society for Testing and Materials, Philadelphia, 1987, p. 628.